

FIG. 1. Energy diagram for the  $\nu P_2(37)$  and  $\nu Q_1(37)$  transitions. The calculated intensity pattern of the  $\nu P_2(37)$  doublet may be compared with the observed transitions  $\nu P_2(37)$  and  $\nu P_2(36)$ .  $\nu Q_1$  transitions are reported in Ref. 3.

presents the  $K$  doubling considering asymmetry and centrifugal distortion splitting. For both sets of levels, the allowed transitions are indicated: i.e.,  $\nu P_2(37)$  and  $\nu Q_1(37)$ . While the pattern of the  $\nu P_2(37)$  doublet is reversed for the two cases [Figs. 1(a) and 1(b)] only an alternation in the splitting of the  $\nu Q_1(37)$  doublets is noticed. In an observed  $\nu P_2(J_{K_a K_c})$  doublet the two components have different statistical weights. If  $K_c$  is odd (even) then the higher frequency component is stronger (weaker). This is illustrated on the bottom of the figure, where oscilloscope tracings of the  $\nu P_2(37)$  and  $\nu P_2(36)$  transitions are shown. The intensity pattern weak, strong; strong, weak for increasing frequency is clearly visible and may be compared with the calculated pattern.

During the course of this work some additional hitherto unmeasured transitions of the  $K=1\leftarrow 0$  and  $K=2\leftarrow 1$  rotational subbands have been assigned. The molecular constants quoted in Paper IV predicted accurately all newly assigned transitions to within 0.90 MHz. The previously reported 140 rotational transitions fit to an eight parameter expression (three rotational constants and five centrifugal distortion constants) with a standard deviation of 0.15 MHz, and therefore we have refrained from reanalyzing the new data. Only a marginal improvement of the rotational constants can be expected.

It should be noted however, that a similar  $K$  doubling to the one observed for the  $K=\pm 2$  levels of HSSH and DSSD occurs in symmetric top molecules as well. This has been found for the  $K=\pm 3$  and  $K=\pm 6$  levels of ammonia,<sup>4,5</sup> and recently this splitting of the  $K=\pm 3$  levels of phosphine has been observed in the radio frequency spectrum of that molecule.<sup>6</sup>

The author would like to acknowledge a fellowship from the Deutsche Forschungsgemeinschaft.

\* Present Address: Max-Planck-Institut für Radioastronomie, Argelanderstraße 3, 53 Bonn, West Germany.

<sup>1</sup> G. Winnewisser, J. Chem. Phys. **56**, 2944 (1972).

<sup>2</sup> G. Winnewisser and P. Helminger, J. Chem. Phys. **56**, 2954 (1972).

<sup>3</sup> G. Winnewisser and P. Helminger, J. Chem. Phys. **56**, 2967 (1972).

<sup>4</sup> W. E. Good and D. K. Coles, Phys. Rev. **71**, 383 (1947).

<sup>5</sup> E. Schnabel, T. Törring and W. Wilke, Z. Physik **188**, 167 (1965).

<sup>6</sup> P. B. Davies, R. M. Neumann, S. C. Wofsy, and W. Klemperer, J. Chem. Phys. **55**, 3564 (1971).

### Third Virial Coefficients and Nonadditivity in Argon and Neon

C. H. J. JOHNSON AND T. H. SPURLING

CSIRO Division of Applied Chemistry, G.P.O. Box 4331, Melbourne, Victoria 3001, Australia

(Received 15 March 1972)

Siska, Parson, Schafer, and Lee<sup>1</sup> have recently published details of intermolecular potentials for argon<sup>1</sup> and neon.<sup>2</sup> The neon potential will be referred to as MSV (Ne) and the argon potentials as MSV II (Ar)

and MSV III (Ar). In these potentials the repulsive parts have been determined very accurately from crossed beam differential elastic scattering measurements while the attractive dispersion parts have been

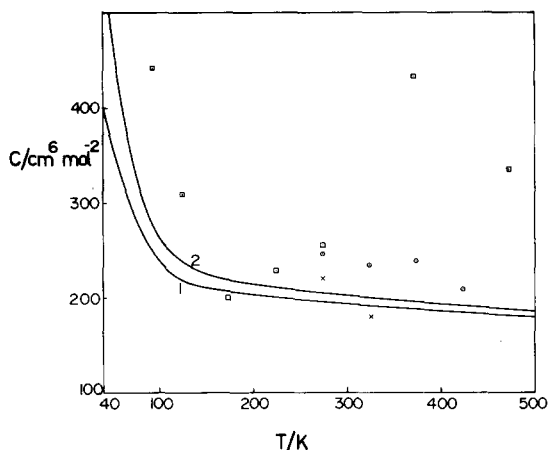


FIG. 1. Comparison of computed and experimental third virial coefficients for neon.  $\circ$ , A. Michels, T. Wassenaar, and P. Louwse, *Physica* **26**, 539 (1960);  $\square$ , C. A. Crommelin, J. P. Martinez, and H. Kamerlingh Onnes, *Commun. Phys. Lab. (Leiden)* **154a** (1919);  $\times$ , G. A. Nicholson and W. G. Schneider, *Can. J. Chem.* **33**, 589 (1955); 1, additive third virial coefficients for MSV (Ne); 2, Total third virial coefficient for MSV (Ne) with all terms up to and including the triple quadrupole terms. For neon terms past the triple dipole term make only a small contribution to the third virial coefficient.

obtained from the results of quantum mechanical calculations. These potential functions have thus been determined independently of virial coefficient data and so provide a means of assessing nonpairwise additivity effects in the third virial coefficient.

Accordingly, we have computed values of the classical third virial coefficient for neon and argon using these potentials, first with the additive form of  $C(T)$  and then in the nonadditive form first for nonadditivity due to the triple dipole term alone and second for nonadditivity due to all the multipole terms up to the triple quadrupole term.<sup>3</sup> The results for neon are shown in Fig. 1 and the results for both argon potentials in Fig. 2. In all these computations we have used Lahiri and Mukherji's estimates of the quadrupole polarizability.<sup>4</sup> Quantum corrections to the third virial coefficient of neon are expected to become important below a reduced temperature of about 2.0 (91.7°K). This is outside the experimental range.

As can be seen from Fig. 1 nonadditivity effects arising from the multipole terms do not contribute

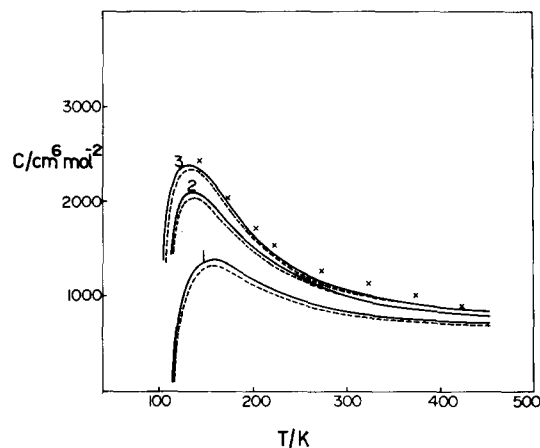


FIG. 2. Comparison of computed and experimental third virial coefficients for argon.  $\times$ , A. Michels, Hub. Wijker, and H. K. Wijker, *Physica* **15**, 627 (1949); 1, Additive third virial coefficients for MSV II (Ar) (broken line) and MSV III (Ar) (full line); 2, Third virial coefficients with only the triple dipole non-additive term; 3, third virial coefficients with nonadditive terms up to and including the triple quadrupole term.

significantly to the third virial coefficient for neon and furthermore the scatter in the experimental data makes it difficult to estimate any possible effects of repulsive nonadditivity. The most one can say is that the computed results agree with experiment within the possible experimental error, which is obviously quite large.

However, for argon Fig. 2 shows that the dispersion nonadditivity effects are significant and that the repulsive nonadditivity effects must be quite small, in agreement with our earlier conclusion<sup>5</sup> concerning the Barker-Pompe potential for argon. The calculated results with multipole nonadditivity agree with experiment to within the uncertainty, which may be as large as  $\pm 10\%$ . More precise experimental measurements of third virial coefficients would be of great value.

<sup>1</sup> P. E. Siska, J. M. Parson, T. P. Schaefer, and Y. T. Lee, *J. Chem. Phys.* **55**, 5762 (1971).

<sup>2</sup> J. M. Parson, P. E. Siska, and Y. T. Lee, *J. Chem. Phys.* **56**, 1511 (1972).

<sup>3</sup> R. J. Bell, *J. Phys. B* **3**, 751 (1970).

<sup>4</sup> J. Lahiri and A. Mukherji, *Phys. Rev.* **155**, 24 (1967), and references contained therein.

<sup>5</sup> C. H. J. Johnson and T. H. Spurling, *Australian J. Chem.* **24**, 2205 (1971).

## EPR Line Shapes of Polycrystalline Ammonium Aluminum Alum: $\text{VO}^{2+}$

P. A. NARAYANA AND K. V. L. N. SASTRY

*Department of Physics, University of New Brunswick, Fredericton, New Brunswick, Canada*

(Received 28 February 1972)

In order to extract maximum and precise information from electron paramagnetic resonance spectrum it is desirable to use single crystals. However it is not always possible to obtain sufficiently large single crystals. This

is particularly true with biological systems such as metal proteins, and then one is restricted to the use of samples with random orientations of paramagnetic complexes. It is however obvious that except in the